Biol. Cybern. 74, 487–495 (1996)

Biological Cybernetics

# Coordination of side-to-side head movements and walking in amphetamine-treated rats: a stereotyped motor pattern as a stable equilibrium in a dynamical system

**Neri Kafkafi**[1], **Stavit Levi-Havusha**[1], **Ilan Golani**[1], **Yoav Benjamini**[2]

[1] Department of Zoology, George S. Wise Faculty of Life Sciences, Tel-Aviv University, Tel-Aviv, Israel
[2] Department of Statistics, Tel-Aviv University, Tel-Aviv, Israel

Received: 18 May 1995/Accepted in revised form: 19 December 1995

**Abstract.** Rats injected with 5.0 mg/kg (+)-amphetamine perform, at one stage of the drug's influence, rhythmic side-to-side head movements while walking. This makes them an interesting preparation for investigating how stereotyped motor patterns emerge from the coordination of periodic movements. We report here such a pattern we have isolated: the left foreleg and the right hindleg land on the ground as the head reaches the peak of its movement to the right, and vice versa (contra-lateral pattern). We show that this pattern can be explained as a stable equilibrium in a simple, nonlinear dynamical model, similar to models developed for tapping with both hands in human subjects. The model also accounts for sequences of behavior that are *not* in the contra-lateral pattern, explaining them as a flow of the system back towards the stable equilibrium after a disturbance.

Motor patterns that constitute the building blocks of unconstrained behavior are often defined as fixed phase relations between movements of the parts of the body. This study applies the paradigm of Dynamic Pattern Generation to free (unconstrained) behavior: motor patterns are defined as stable equilibria in dynamical systems, assembled by mutual influence of concurrent movements. Our findings suggest that this definition is more powerful for the description of free behavior. The amphetamine-treated rat is a useful preparation for investigating this notion in an unconstrained animal whose behavior is still not as complex and variable as that of the normal animal.

## 1 Introduction

### *1.1 Application of Dynamic Pattern Generation to free and drug-induced motor behavior*

The idea that stereotyped motor patterns could be best understood and modeled as stable equilibria, or attractors, in open (dissipative) dynamical systems has been termed Dynamic Pattern Generation (Schoner and Kelso 1988). Having its origins in the pioneering work of von Holst (1937), it is now well established and has both a theoretical basis (Kugler et al. 1980; Schoner et al. 1986; Kugler and Turvey 1987; Schoner 1993) and experimental applications in various systems and levels (e.g., Yamanishi et al. 1980; Tatsumi and Suzuki 1983; Haken et al. 1985; Tuller and Kelso 1989; Dijkstra et al. 1994).

A typical experimental model is that of human subjects required to tap rhythmically with the index fingers of both hands. The reader can immediately find by experiment that there are only two convenient phase relations between the hands: the in-phase relation (both hands tap simultaneously) and the anti-phase relation (hands tap alternately in half a cycle difference). This property, and others of the tapping experiment, are predicted by dynamical models of two coupled oscillators. In these models, the stereotyped motor patterns (in-phase and anti-phase) can be shown to emerge as stable equilibria: states to which the system is attracted from nearby states (Yamanishi et al. 1980; Haken et al. 1985).

As ethologists we are tempted to try applying Dynamic Pattern Generation to the problem of description of free (unconstrained) behavior. This problem is critical not only in ethology, but also in other areas, e.g., in tests of 'open field behavior', which are used in neuroscience and behavioral pharmacology to measure the effects of different manipulations in the central nervous system. Such application, however, is far from being straightforward. Free motor behavior is extremely complex and variable, comprised of many degrees of freedom, and the relevant variables are usually not known in advance. Moreover, because of the highly nonlinear nature of the problem, it is unlikely that the complex case of free behavior could be described as a combination of many simplified cases.

One good strategy for approaching this problem might be by starting from the description of drug-induced behavior, which is typically more stereotyped

---

*Correspondence to:* N. Kafkafi

and predictable. Drug-induced behavior could serve as a step between precise but simplified experimental models such as the tapping experiment, and the complex movement of the normal animal. This study could also be of use to pharmacologists and neurobiologists interested in measuring the effect of these drugs on open field behavior.

We describe here a stereotyped motor pattern, discovered by us in the unconstrained, open field behavior of laboratory rats injected with 5.0 mg/kg (+)-amphetamine. We will show that this motor pattern can be understood as a stable equilibrium in a simple, discrete dynamical system. We will also demonstrate the advantages of this dynamic description over the conventional description of drug-induced behavior.

### *1.2 Concurrent periodic movements in rats injected with 5.0 mg/kg amphetamine*

Adani et al. (1991) investigated the behavior of rats injected with 5.0 mg/kg amphetamine, using the Eshkol-Wachman Movement Notation (EW). They found that its development could be described as the superimposition of two independent processes: (i) forward walking is first enhanced and then eliminated, (ii) lateral movements appear, first of the head and then spreading along the trunk in a cephalo-caudal order. Different individual profiles of unfolding of the behavior can be explained as different timings between these two processes. It follows that some of the rats are still walking as they start moving their heads (and later also the upper and lower torso) rhythmically from side-to-side. These rats perform two kinds of periodic movements (walking and side-to-side head movements) simultaneously. The question we study here is how they coordinate these two movements and how stable motor patterns emerge from this coordination.

## 2 Methods

### *2.1 Injection and observation procedures*

The experimental animals were nine laboratory rats, males and females, of the 'hooded' strain, weighing 200–400 g. They were grouped and housed with free access to food and water in 35 × 50 × 20 cm cages, 1–5 rats per cage. All rats were experimentally naive and were tested once. They were injected subcutaneously with 5.0 mg/kg (+)-amphetamine and immediately placed on the observation platform. The observation platform was a 120 × 140 cm flat sheet of glass, placed horizontally about 2 m above the ground. A large mirror was placed underneath the observation platform, tilted at 45° to it, to allow videotaping of a view of the animals from below. In previous experiments (e.g., Eilam and Golani 1988; Szechtman et al. 1985; Adani et al. 1991) it was found that this view allowed an accurate evaluation of the horizontal orientation of the head and trunk, and the direction and timing of stepping of all four legs.

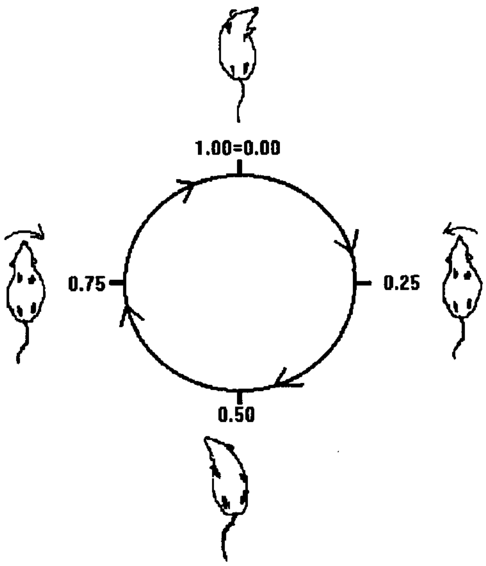

**Fig. 1.** The cycle of side-to-side head movement, as defined in the present study. The four phases which are illustrated in the figure ($\phi = 0.25$, $\phi = 0.5$, $\phi = 0.75$ and $\phi = 1 = 0$) were measured directly. The rat is seen from below, as observed in the video record. Right and left are relative to the observer when the rat is facing 'up'

All the rat's behavior during 1.5 h following the injection was videotaped at 25 frames/s, and a time display was added to the video record by a time-code generator.

### *2.2 Measurement of head movement and stepping coordination*

The coordination between head movement and stepping was analyzed frame by frame, using a videotape with a still mode.

For measuring the periodic side-to-side head movements (head cycle) we used the angle between the head and the torso. The phases in which the head reaches the peak of its movement to the right or to the left, and in which it is in line with the torso, are easy to discern on the video record. For this reason we defined $\phi$, the phase of the head cycle, as proceeding from 0 to 1 (Fig. 1), where 0 denotes the peak of its movement to the right, 0.25 denotes alignment with the torso while moving to the left, 0.5 the peak to the left, 0.75 alignment with the torso while moving to the right, and 1 is again the peak to the right (equal to 0). The observer recorded the frames in which these four phases occurred, and the phase in the frames between them was computed by simple linear interpolation. The observer also recorded the timing (in frames) of establishment and release of foot contact with the ground in all four legs.

Since we were interested in the coordination between the two periodic movements – the head cycle and the walking (stride cycle) – we clearly had to screen the behavior for the sequences where these two cycles coexisted. For this reason, analysis was performed on only five of the nine rats, who still showed substantial forward progression during the stage of rhythmic side-to-side head movements. At this stage the rats developed the stereotyped locomotor paths typical with 5.0 mg/kg amphetamine, usually circling the observation platform along its edges (Schioring 1971), or walking back and forth between two corners along the same edge while moving their head rhythmically from side to side (stage III in Adani et al. 1991).

From the sequences of Adani's stage III we excluded all the instances in which the head cycle or the stride cycle were not regular, so that their phase could not be defined. Regularity of the head cycle was defined as going from 0 to 0.25, 0.5, 0.75 and 0 again in that order, with no stopping for more than three frames (0.12 s) in one phase. Regularity of the head cycle was not preserved (i) when the rat turned at the corners of the observation platform. Also, (ii) at the beginning of stage III some of the rats performed the head movements to only one side.

Regularity of the stride cycle was defined as walking in the diagonal order. Since the model presented here refers only to the landings of the forelegs, we actually include all strides in which the right and left forelegs step alternately. This regularity was not preserved (i) when turning at corners and (ii) in rare instances of stopping.

The recorded data practically include every sequence of more than two succeeding strides that passed the criteria above. Since the duration of stage III was different in individual rats, sample size was also different. The number of strides recorded for rats 1 to 5 was, respectivley, 41, 71, 150, 101 and 69. All the analysis in Sect. 3 is performed and presented for each rat separately.

The rather strict criteria above were needed to screen the behavior for data that are convenient for investigating the coordination between the head cycle and the stride cycle. It is important to stress however, that the phenomena that will be reported in Sect. 3 were also prominent in many sequences that failed some of the criteria. These criteria, however, do not restrict in any way the *phase relation* between the two cycles.

### 2.3 Statistical methods

Several distributions, such as the distribution of $\phi$, are studied and displayed using density curves. Each density was estimated using a kernel density estimator with gaussian kernel, using the implementation in the statistical software S (Becker et al. 1988).

For the purpose of estimating nonparametrically the dependence of one variable on the other, the lowess method, as implemented on the same statistical software, is used. This method employs local linear regression in the neighborhood of each point separately to yield the predicted value for the dependent variable. The participating points at each location have higher weights the closer they are to the point at which the relationship is estimated. Further automatic downweighting of outliers assures the robustness of this procedure. For more details about the lowess method see Cleveland (1979).

## 3 Results

### 3.1 Observed properties of head and stepping coordination

In the five rats that still walked forward when side-to-side head movements appeared, we observed a typical pattern of head and stepping coordination: the left foreleg and the right hindleg landed when the head was approximately at the peak of its movement to the right, and then the right foreleg and left hindleg landed when the head reached the peak of its movement to the left (Fig. 2). The hindlegs landed simultaneously with the diagonal foreleg or a little (1–3 frames) after them. We termed this pattern the *Contra-Lateral Pattern* (CLP). It tended to appear when the rat walked in a straight line. Many times the rat lost the pattern for a few head cycles, and then 'locked' again. When the rat turned at the corners of the observation platform, the CLP was always lost, as the head cycle stopped during the turn. Usually the rat resumed the CLP after completing the turn and walking again in a straight line. In some sequences the CLP was very prominent and persistent, especially when there were regular and large-amplitude head movements, while in others it was more difficult to recognize.

Figure 3 displays the density functions of $\phi_R$, the head phase when the right foreleg landed, and $\phi_L$, the head phase when the left foreleg landed, in the five rats. In all rats, the right foreleg preferentially landed when the head was at peak left ($\phi = 0.5$) and the left foreleg preferentially landed when the head was at peak right ($\phi = 1.0$). This preference was not very prominent, however, except in rat 3, and there are many landings in other head phases also.

When the rat is in the CLP there is a fixed phase relation of 1:1 between the head cycle and the stride cycle. When the rat loses the pattern, however, it almost always performs more than one stride per head cycle: the legs are, so to speak, faster than the head (alternatively, the head lags behind the legs). This phenomenon in the

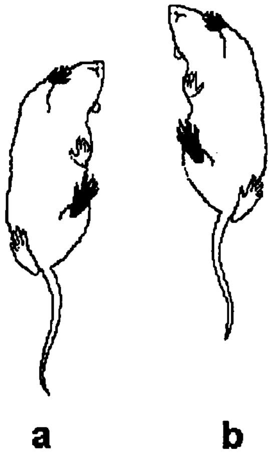

**Fig. 2a, b.** Two phases of the Contra-Lateral Pattern as seen in the video record. The rat is seen from below. Paws at the time of landing are marked with black. **a** Head at peak right; left foreleg and right hindleg are landing. **b** Head at peak left; right foreleg and left hindleg are landing. Right and left are relative to the observer when the rat is facing 'up'

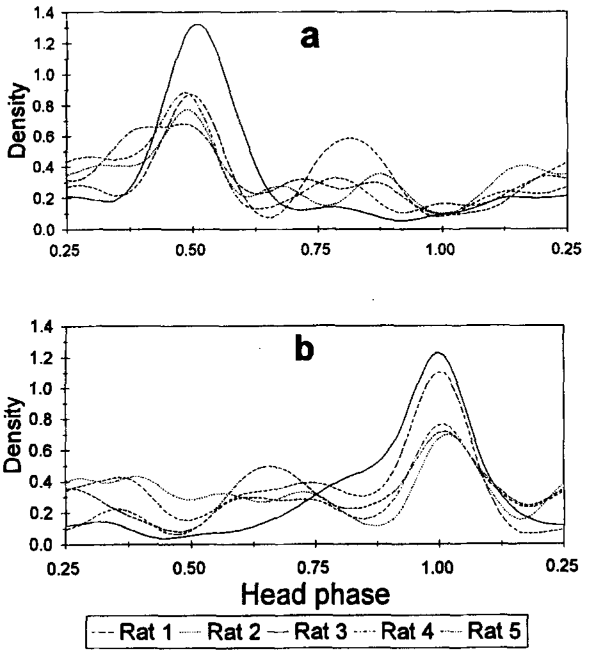

**Fig. 3.** Density functions of $\phi_R$, the head phase at the instant of landing of the right foreleg (**a**), and $\phi_L$, the head phase at the instant of landing of the left foreleg (**b**), in the five rats. The sample size for each leg in rats 1 to 5 is, respectively, 41, 71, 150, 101 and 69

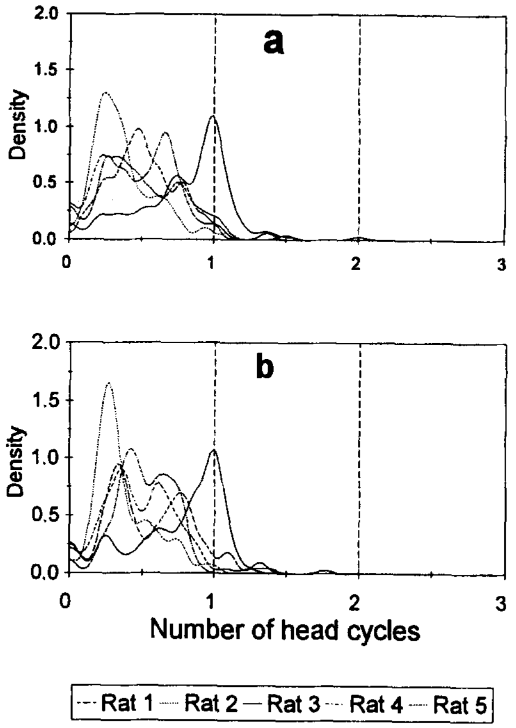

**Fig. 4.** Density functions of the number of head cycles between successive landings of the right foreleg (**a**) and between successive landings of the left foreleg (**b**). The sample size for each leg in rats 1 to 5 is, respectively, 41, 71, 150, 101 and 69

phase relation between two cycles was termed *relative coordination* by von Holst (1937). To see this we measured how many head cycles elapsed between successive landings of the same foreleg (i.e., one stride). These density functions are displayed in Fig. 4. In rat 3, which showed a very prominent CLP, there are many stride cycles that extend over one head cycle. In the other rats, which had a higher tendency to 'lose' the CLP, most strides extend over less than one head cycle. There are, however, almost no stride cycles that extend over *more* than one head cycle. In rat 3, a sharp decline in the density can be seen after 1:1 head cycles.

This phenomenon can not be attributed to simple mechanical limitations of the rat's body, i.e., that the sideways movement of the head must pull the foreleg with it. The angle of the head relative to the torso hardly ever exceeded 45°, and the side-to-side movement of the rat's body was also usually much smaller than 45°. Rats are anatomically much more flexible, as is illustrated by rats recovering from lesions to the lateral hypothalamus, who perform extremely large lateral movements of the head and torso whilst maintaining foot contact with the ground (Golani et al. 1979).

### *3.2 Model*

In this section we present a simple dynamical model that accounts for the observed features of head and leg coordination. The model was constructed according to the modeling strategy of Dynamical Pattern Generation, in particular models of the tapping experiment (Yamanishi et al. 1980; Haken et al. 1985; Schoner et al. 1986). This strategy is to find a good 'order parameter', i.e., a collective variable that has well-defined dynamics. The observed motor pattern is then explained as a stable equilibrium (attractor) in the state space of the order parameter, and other observed properties of the coordination may be explained by the dynamics of the state space. Following this strategy, we explain in the present study on observed phenomenon of relative coordination by a dynamical property termed intermittency, as suggested by Kelso and Ding (1993) and Schoner (1993).

We should, however, point out an important difference between this and previous studies, not so much in the modeling process itself as in the motivation behind it. The motivation of the workers cited above is to reveal how the nervous system controls and coordinates movement. In order to construct elegant, explicit and powerful models, they employ well-controlled experimental setups and only two degrees of freedom (states of the right and left fingers), from which the order parameter (the fingers' relative phase) is constructed in a rather simple way.

As ethologists, however, our first interest is in the description of the free movement of the whole animal in a natural noisy and hard-to-control environment. This implies handling as large a number of degrees of freedom as possible, and the number of low-dimensional order parameters that can be constructed from them rises very fast. Moreover, *a priori* assumptions become harder to make (as, for example, how the head cycle affects each of the foreleg cycles). Therefore, the main criterion is how well defined the empirical behavior of the order

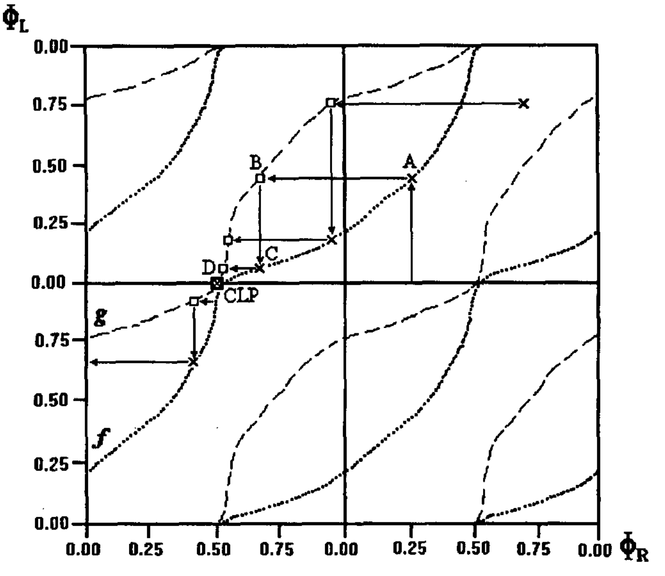

Fig. 5. A phase-plane representation of the model behavior. It consist of four replicas of the phase-plane of $\phi_R$ and $\phi_L$, tiled 2 × 2. The curves $f$ and $g$ are suggested according to conditions c1, c2 and c3. Vectors illustrate the flow of the system (see text for details)

parameter is. In this study, we measured five degrees of freedom (cycles of the four legs and of the head). We have tried several possibilities, and arrived at the model presented here, which uses three of the five degrees of freedom to construct a two-dimensional state space. We are currently looking for even better order parameters which consider also the hindleg landings as well as the release of contact with the ground of all four legs.

The model assumes that $\phi_R$, the landing phase of the right foreleg *relative to the head cycle*, determines the next landing phase of the left foreleg $\phi'_L$, again measured relative to the head cycle. That is:

$$\phi'_L = f(\phi_R) \qquad (1)$$

and the landing phase of the left foreleg determines the next landing phase of the right foreleg:

$$\phi'_R = g(\phi_L) \qquad (2)$$

Again, all phases are measured relative to the head cycle.

This assumption is similar to the one used in the models by Yamanishi et al. (1980) and Haken et al. (1985). The main difference is that in our model the landing (= tapping) phase of each forelimb is measured relative to the head cycle, and not relative to the other limb cycle. In this way, a third degree of freedom (the head cycle) is included.

The two difference equations, (1) and (2), comprise a simple, discrete dynamical system that can be plotted in the phase-plane of the two variables, $\phi_R$ and $\phi_L$ (Fig. 5). Note that, since both variables are cyclic, the topology of the phase-plane is that of a torus. ($\phi = 1$ is also $\phi = 0$, so that the upper edge of the phase-plane is also the bottom edge, and the right edge is also the left edge. To create the torus, make first a cylinder by 'gluing' the right edge to the left edge, then close the cylinder to a torus by 'gluing' together top and bottom edges.) In order to see the continuity of the phase on a flat page, the graph in Fig. 5 is comprise of four replicates of *the same* phase-plane, with left edges glued to right edges and top edges to bottom (see Winfree 1980 for the use and applications of such representations).

Every point designated by a cross in Fig. 5 describes a landing of the right foreleg and then a landing of the left foreleg, at the head phases specified by the coordinates of the point. Every open square describes a landing of the left foreleg and then a landing of the right foreleg. The point (0.5, 0.0), marked CLP in Fig. 5, represents the Contra-Lateral Pattern: right foreleg lands when the head reaches peak left, and left foreleg lands when the head reaches peak right.

A hypothetical case of the functions $f$ and $g$ is plotted in Fig. 5. (Note that for $g$ the independent axis is the *vertical* axis, and the dependent axis is the horizontal axis.) We do not have to know $f$ and $g$ precisely. We assume only three qualitative conditions, demonstrated by the curves drawn in Fig. 5: (c1) $f$ and $g$ are, in general, rising; (c2) $g$ is above and to the left of $f$ in most parts of the phase-plane; (c3) in the region of the CLP state, $f$ and $g$ are closer to each other. To simplify the following discussion we will assume that $f$ and $g$ are exactly tangent in the CLP area, but later we will show that they may also intersect, or only get close to each other, without much influence on the model's predictions.

As we will demonstrate in the following discussion, c3 accounts for the observable abundance and stability of the CLP, while c2 accounts for the relative coordination between the head cycle and the stride cycle condition. c1 follows directly from the definition of $f$ and $g$: it states only that if the landing of one foreleg occurs later, relative to he head cycle, then the *next* landing of the other foreleg will generally also occur later, relative to the same head cycle.

Conditions c2 and c3 imply that *at least* one of the functions $f$ and $g$ is nonlinear, because two straight lines can not be closer to each other in one area if in other areas one of them is always far to the same side. Also, the parameters of $f$ and $g$ are not known exactly. Nonetheless, the qualitative behavior of the model can be deduced from the phase-plane in Fig. 5, using the graphic methods of iterative map analysis (for qualitative methods in nonlinear discrete dynamical systems see, e.g., Sandefur 1993 or Baker and Gollub 1990). Suppose, for example, that the right foreleg lands when the head is straight ahead in relation to the body and moving to the left ($\phi = 0.25$). To find when the left foreleg will land next, draw a vertical line from $\phi_R = 0.25$ and check where it intersects $f$ (point A in Fig. 5). To find when the next landing of the right foreleg will be, draw a horizontal line and see where it intersects $g$ (point B in Fig. 5). If we continue to solve (1) and (2) recursively by this graphical method (points C, D), we find that we reach the CLP point, and then stay there, because at this point $f$ and $g$ meet. It is easy to see that in this manner we reach the CLP state and stay there from every point in the phase-plane (which represents every possible coordination between head cycle and foreleg landings). This means that the CLP state is a *stable equilibrium* in the model. Note, however, that when the system is at the CLP state, any small fluctuation that takes it to the left and/or down from the CLP will cause it to be repelled further down and to the left, until it reaches the CLP again from above. The CLP state is, then, stable from above and *unstable* from below.

The model accounts for the two observable properties of head-foreleg coordination mentioned in Sect. 3.1. The first, the abundance of the CLP, is clearly explained by its attraction and stability. The second property is that the duration of the stride cycle is equal to, or smaller than, the duration of the simultaneous head cycle. In the model, this happens because $g$ is above and to the left of $f$ in most parts of the phase-plane, so that after a fluctuation the system always flows down and to the left (Fig. 5). This means that *the next landing of the same foreleg is at an earlier phase*, i.e., after less than one head cycle. Once the system reaches the stable state again, the phase of the next landing is the same, i.e., the duration of the stride cycle is precisely one head cycle.

The system as shown in Fig. 5, with $g$ and $f$ exactly tangent, is *structurally unstable* (this concept should not be confused with the concept of stability in the phase-plane discussed above). It means that the (unknown) parameters of $f$ and $g$ must be infinitely accurate in order to preserve the tangency between $f$ and $g$ – an unlikely situation in practice. Almost any small change of these parameters will change $f$ and $g$ to one of two structurally stable situations: (s1) $f$ and $g$ only get close to each other in the CLP region, but do not touch each other (Fig. 6b); (s2) $f$ and $g$ intersect at two (or any even number of) close points in the CLP region (Fig. 6c).

However, because of the high level of noise in the real case, due to both external disturbances and inaccuracy of measurement, these situations will not change the model predictions: In situation s1 the place where $f$ and $g$ get closer will function as a 'bottle neck', slowing down the system flow so that it is insignificant relative to the noise level (Fig. 6b). This phenomenon is known as 'type I intermittency' (Baker and Gollub 1990) and was suggested as an explanation of von Holst's relative coordination by Kelso and Ding (1993). In situation s2 (Fig. 6c) the right upper point of the intersection would be stable equilibrium from above *and* below, and the left lower intersection point would be *unstable equilibrium* (any nearby state would be repelled from it). This means that with no fluctuations the system will reach the stable intersection point and stay there, but any small fluctuation taking it left or down beyond the unstable intersection point will cause it to flow further left and down, until it will reach again the stable intersection point from right and above, losing one head cycle in the way. The exact parameters of $f$ and $g$ are not important, then, as long they satisfy conditions c2 and c3.

Condition c1, which had been formulated quite generally before, should also be formulated in more exact terms. It is easy to verify graphically that the model's qualitative behavior stays as above even if $f$ and $g$ are not rising in a complete monotonous way, but also descend in parts of their range. The more exact condition is, therefore, that they do not have local minima that are lower than the previous CLP point. Note, however, that even if this condition is not fulfilled, the model's behavior still may not change very much if the exceptions are small.

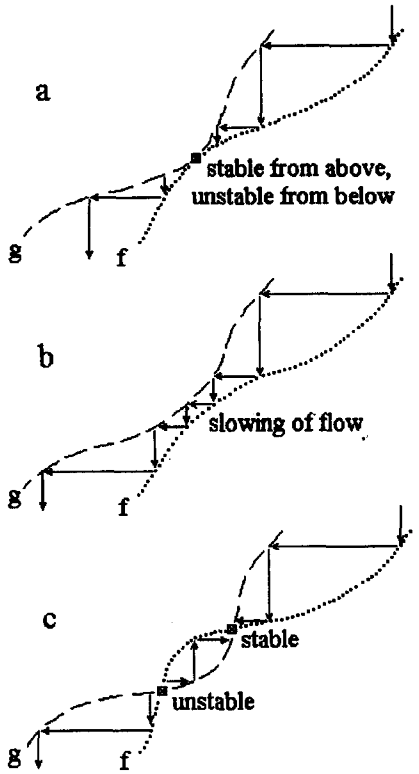

**Fig. 6.** **a** A structurally unstable situation, with $f$ and $g$ exactly tangent. The equilibrium state at the point of tangency is stable from the right and above and unstable from the left and below. After a small change in the parameters of $f$ and $g$, one of two structurally stable situations (**b**, **c**) is likely to occur. **b** There is slowing of the flow but no equilibrium point. **c** There are two equilibrium states at the intersections of $f$ and $g$, where the upper is stable and the lower is unstable

### 3.3 *Estimation of f and g*

Although the method of measurement applied in this study was relatively simple and of low accuracy, it was possible to estimate $f$ and $g$ from the data, and to show that they satisfy conditions c1, c2 and c3. The landing phase of each foreleg in these sequences was plotted against the previous landing phase of the other foreleg. Figure 7 displays the plot of $\phi'_L$ vs $\phi_R$ in rat 4. Figure 8 displays the plot of $\phi'_R$ vs $\phi_L$ in the same rat (the graphs are replicated and tiled as in Fig. 5, in order to show the continuity). Note that data points tend to pile up in the region of (0.5, 0.0), the CLP area.

The nonlinear relationship between $\phi'_L$ and $\phi_R$ in the diagonal band is estimated in the following way: First, $\phi'_L$ and $\phi_L$ are transformed by $x = \phi'_L + \phi_R$, $y = \phi'_L - \phi_R$ to create a horizontal band. Then, the nonlinear dependency of $y$ and $x$ is estimated using the lowess method detailed in Sect. 2.3, yielding $\hat{y}(x)$. Finally,

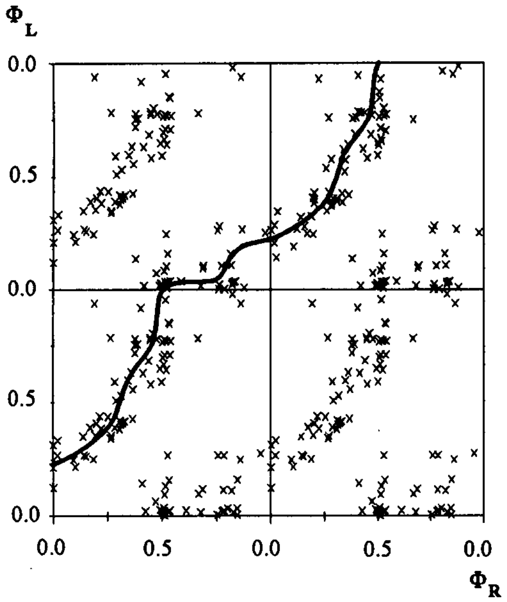

Fig. 7. $\phi_L$, the head phase of the left foreleg landing, as a function of $\phi_R$, the head phase of the previous landing of the right foreleg, in rat 4. The graph is replicated and tiled as in Fig. 5, to show continuity. The number of data points (before replicating) is 101. An estimated curve for $f$ is shown for one of the repetitions

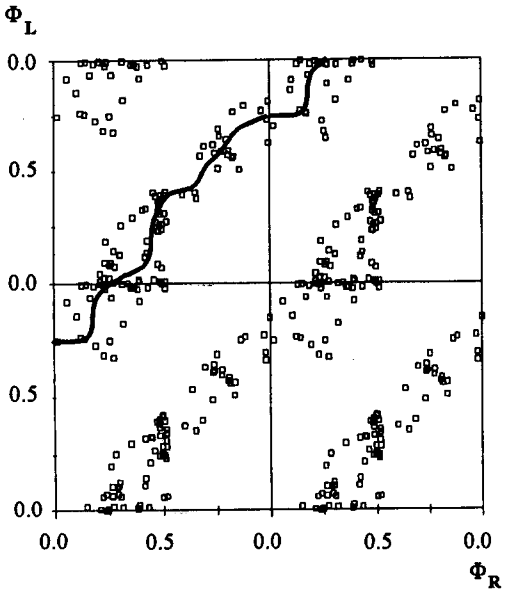

Fig. 8. $\phi_R$, the head phase of the right foreleg landing, as a function of $\phi_L$, the head phase of the previous landing of the left foreleg, in rat 4. Note that the independent axis is the vertical axis. The graph is replicated and tiled as in Fig. 5. The number of data points (before replicating) is 101. An estimated curve for $g$ is shown for one of the repetitions

the pair $x$, $\hat{y}(x)$ is transformed back to $\phi_R$, $\hat{f}(\phi_R)$. The estimated $f$ is given by the smooth curve in Fig. 7. The function $\hat{g}$ is estimated from $\phi_R'$ and $\phi_L$ using the same procedure, and is given by the smooth curve in Fig. 8.

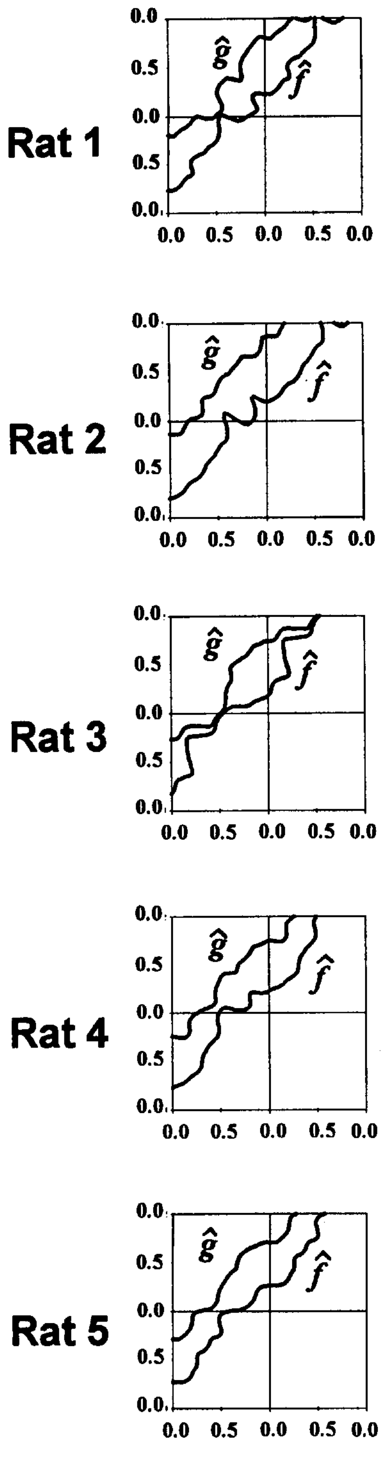

Fig. 9. Estimated curves $\hat{f}$ and $\hat{g}$ for the five rats. The graphs are replicated and tiled as in Fig. 5

Figure 9 displays the estimated curves for $g$ and $f$ for the five rats. Compare these with the hypothetical shape of $f$ and $g$ in Fig. 5. In all rats, $\hat{g}$ is above and to the left of $\hat{f}$, and they are closest to each other in the CLP area. Since our estimation method employed smoothing necessary for reducing the effect of noise, the functions are probably closer to each other in the CLP area than the estimated curves indicate.

## 4 Discussion

### *4.1 The relevance of a dynamic definition of motor patterns to free behavior*

The description of free (unconstrained) behavior is the basis for the scientific disciplines of ethology and behavioral neuroscience. In these disciplines, a motor pattern, whether single or repetitive, is usually defined as *a fixed, stereotyped coordination* between movements of the participating parts of the body. In other words, whenever the definition of a pattern involves more than one kinematic degree of freedom $df_1$ $df_2$, . . . , this definition would say something like: 'when $df_1$ is doing $x$, $df_2$ is doing $y$, . . . .' In this study, for example, the CLP could be defined as a specific, fixed phase relation between the stride cycle and the head cycle: 'when the left foreleg lands on the ground, the head reaches the peak of its movement to the right, and vice versa.' Any deviation from this fixed coordination would then be considered as statistical noise (Barlow 1977; Schleidt 1974). When deviations are too large, as is often the case with free behavior (see again the densities in Fig. 3), the definition of the pattern becomes more and more problematic, and the pattern become less and less suitable for the measurement of behavior. This is why many of the disciplines belonging to behavioral neuroscience avoid a precise definition of motor patterns, so that these patterns (e.g. 'fixed action patterns in ethology, 'response categories' in behavioral pharmacology) can be recognized only *subjectively* by 'experienced observers,' 'as in the judgements of works of art' (Beer 1980). This is why we consider the problem of definition and recognition of motor patterns as fundamental for ethology and behavioral neuroscience.

The new theory of Dynamical Pattern Generation suggests, however, an alternative way for defining motor patterns: *A specific pattern is defined by a dynamical system (i.e., a vector field) in the space of the relevant variables* (Kugler et al. 1980; Schoner and Kelso 1988). The stereotyped situations of fixed phase relations are stable equilibrium points (or more complex kinds of attractors) in this space, but other situations may also be recognized as belonging to the pattern if their plot in the state space matches the flow of the vector field (e.g. the vectors in Fig. 5). This dynamic definition is more powerful than the old, static definition. For example, in the static definition only the data points in the contra-lateral area in Figs. 7 and 8 would be considered as belonging to the CLP, whereas the dynamic definition can also explain many of the other data points that lie on the curves $f$ and $g$, as points along the flow of behavior in these areas of the state-space. Furthermore, whereas in one of the rats (#3) many successive data points do pile up in the CLP area, thereby demonstrating the stereotypy of the pattern, in the four others the vast majority of data points are *not* located in this area (Figs. 7 and 8 demonstrate it for rat 4). Such 'nonstereotyped' rats nevertheless satisfy the dynamic definition of the pattern, because most of the other data points lie along the flow, on curves that satisfy c2 and c3.

In applying this concept to the description and analysis of unconstrained behavior, our main goal is the *identification of the relevant variables, or 'order parameters'* generating this state-space. These are the variables that have the most well-defined behavior in the state-space. In the present study, this is expressed by the distinctness of the curves $f$ and $g$ created by the empirical data points of the variables $\phi_R$ and $\phi_L$. Other variables we have examined, such as the relative phase of the forelegs (Haken et al. 1985; Suzuki et al. 1980), the relative phase of one foreleg and the head, or the head phase of other events in the stride cycle, showed less ordered structure in the state-space. Since our main motivation has been a low-dimensional description of behavior, this criterion gained priority over simplicity and mathematical explicitness.

This approach of looking for the relevant variables is very similar to the one used in the analysis of normal and drug-induced behavior with EW Movement Notation (Szechtman et al. 1985; Adani et al. 1991; Golani 1992). What is new here is the description of behavior in state-space rather than as a function of time. This type of representation is useful with nonlinear models, which may exhibit a complex behavior arising from a simple topology in state-space.

### *4.2 The relevance of the CLP observed with amphetamine to normal rat behavior*

Typical amphetamine-induced 'stereotypy' has been repeatedly shown to involve the stimulation of dopamine receptors in the striatum (Randrup and Munkvad 1968, 1969), although other biogenic amines have been implicated (Randrup and Munkvad 1964; Arnfeld and Randrup 1968). At the dose used, amphetamine administration may elicit the 5-hyroxytryptamine (5-HT) syndrome (Taylor et al. 1974). The particular phase of drug action including rhythmic side-to-side head movements, in which the CLP is embedded, has been labeled 'head swaying' by Taylor et al. (1974), and assumed to be part of that syndrome. These authors describe head swaying as 'a behavior pattern of fixed topography that is repeated for long periods of time, and which represents an extreme form of natural exploratory head movements and sniffing.'

Is the CLP a single behavior pattern that is merely triggered *en bloc* by amphetamine? This is unlikely, because side-to-side head movements and locomotion have different times of onset with 5.0 mg/kg amphetamine (Adani et al. 1991). They also appear in different proportions with different doses (Taylor et al. 1974).

Since decerebrate animals show impressive ability to perform coordinated motor acts, coordination is usually considered to be mediated at lower levels than the cerebrum. This is especially true for locomotion (Shik and Orlovsky 1976) and for head-foreleg coordination, as in the neck and vestibulo-spinal reflexes (Magnus 1924; Roberts 1978). It would therefore be reasonable to assume that amphetamine induces *separately* both the forward locomotion and the side-to-side head movements. The CLP, a particular head-foreleg coordination, is, however, an emergent property of a dynamic coupling between these two components, and this coupling is mediated at the brain-stem or even spinal cord level. A similar conclusion has been reached by Tuller and Kelso (1989) in their tapping experiment performed with split-brain human subjects. They revealed no effect of the damage on the coupling between the two hands, and concluded that this coupling was mediated at a lower level than the cerebrum.

We hypothesize, therefore, that the CLP may also be found in normal behavior, where it should be sporadic and more vulnerable to external perturbations.

Amphetamine was used in this study as a tool for generating stereotyped behavior. With this drug, several motor patterns are performed intensively and for long periods of time with minimal disturbance, whereas in normal behavior they are less abundant and more disturbed, and therefore much more difficult to measure. In terms of Dynamical System Theory, the drug-induced behavior can be regarded as more autonomous (in the mathematical sense). It is reasonable to hope that stereotypy-inducing psychotrophic agents would enable us to identify relevant key variables that also govern normal, free behavior.

*Acknowledgements.* We thank Prof. Philip Teitelbaum and Prof. Mark Shik for their comments on the manuscript. This research was supported by grant no. 92-00281 from the United States–Israel Binational Science Foundation (BSF), Jerusalem, Israel.

## References

Adani N, Kiriati N, Golani I (1991) The description of rat drug-induced behavior: kinematics versus response categories. Neurosci Biobehav Rev 15:455–460

Arnfeld T, Randrup A (1968) Cholinergic mechanisms in brain inhibiting amphetamine induced behavior. Acta Pharmacol (Copenh) 26:384–394

Baker LG, Gollub JP (1990) Chaotic dynamics: an introduction. Cambridge University Press, Cambridge

Barlow GW (1977) Modal action patterns. In: Sebeok TA (ed) How animals communicate. Indiana University Press, Bloomington, Ind

Becker RA, Chambers JM, Wilks RA (1988) The new S language. Wadsworth and Brooks, Pacific Grove, Calif

Beer CG (1980) Perspectives on animal behavior comparisons. In: Bornstien MH (ed) Comparative methods in psychology. Erlbaum, Hillsdale, NJ

Cleveland WS (1979) Robust locally weighted regression and smoothing scatterplots. J Am Stat Assoc 74:829–836

Dijkstra TMH, Schoner G, Giese MA, Gielen CCAM (1994) Frequency dependence of the action-perception cycle for postural control in a moving visual environment: relative phase dynamics. Biol Cybern 71:489–501

Eilam D, Golani I (1988) The ontogeny of exploratory behavior in the house rat (*Rattus rattus*): the mobility gradient. Dev Psychobiol 21:679–710

Golani I (1992) A mobility gradient in the organization of vertebrate movement: the perception of movement through symbolic language. Behav Brain Sci 15:249–308

Golani I, Wolgin D, Teitelbaum P (1979) A proposed natural geometry of recovery from akinesia in the lateral hypothalamic rat. Brain Res 164:237–267

Haken H, Kelso JAS, Bunz H (1985) A theoretical model of phase transitions in human hand movements. Biol Cybern 51:347–356

Holst E von (1937) Von Wesen der Ordnung im Zentralnervensystem. Naturwissenschaften 25:625–631, 641–647

Kelso JAS, Ding M (1993) Fluctuations, intermittency, and controllable chaos in biological coordination. In: Newell KM, Corcos DM (eds) Variability and motor control. Human Kinetics Publishers, Champaign, Ill

Kugler PN, Turvey MT (1987) Information, natural law and the self-assembly of rhythmic movement. Erlbaum, Hillsdale, NJ

Kugler PN, Kelso JAS, Turvey MT (1980) On the concept of coordinative structure as dissipative structures. I. Theoretical lines of convergence. In: Stelmach GE, Requin J (eds) Tutorials in motor behavior. North-Holland, New York, pp 3–47

Magnus R (1924) Korperstellung. Springer, Berlin Heidelberg New York

Randrup A, Munkvad I (1964) On the relation of tryptaminergic and serotonergic mechanisms to amphetamine induced abnormal behavior. Acta Pharmacol (Copenh) 21:272–282

Randrup A, Munkvad I (1968) Behavioral stereotypies induced by pharmacological agents. Pharmacopsychiatrie Neuro-Psychopharmakol 1:18–26

Randrup A, Munkvad I (1969) Pharmacological studies on the brain mechanisms underlying two forms of behavioral excitation: stereotyped hyperactivity, and rage. Ann NY Acad Sci 157: 928–938

Roberts TDM (1978) Neurophysiology of postural mechanisms, 2nd edn. Butterworth, London

Sandefur JT (1990) Discrete dynamical systems. Clarendon Press, Oxford

Schioring E (1971) Amphetamine induced selective stimulation of certain behavior items with concurrent inhibition of others in an open-field test with rats. Behaviour 39:1–17

Schleidt WM (1974) How fixed is a fixed action pattern? Z Tierpsychol 36:184–211

Schoner G (1993) What can we learn from dynamic models of rhythmic behavior in animals and humans? In: Dynamics and representation in adaptive behavior and cognition. Proceedings of III International Workshop on Artificial Life and Artificial Intelligence, Universidad del Pais Vasco, pp 59–67

Schoner G, Kelso JAS (1988) Dynamic pattern generation in behavioral and neural systems. Science 239:1513–1520

Schoner G, Haken H, Kelso JAS (1986) A stochastic theory of phase transitions in human hand movements. Biol Cybern 53:442–452

Shik ML, Orlovsky GN (1976) Neurophysiology of locomotor automatism. Physiol Rev 56:465–501

Szechtman H, Ornstein K, Teitelbaum P, Golani I (1985) The morphogenesis of stereotyped behavior induced by the dopamine receptor agonist apomorphine in the laboratory rat. Neuroscience 14:783–798

Tatsumi H, Suzuki R (1983) Phase-plane description of crayfish swimmeret oscillator. Biol Cybern 47:59–68

Taylor M, Goudie AJ, Mortimore SA, Wheeler TJ (1974) Comparison between behaviours elicited by high doses of amphetamine and fenfluramine: implications on the concept of stereotypy. Psychopharmacology 40:249–258

Tuller B, Kelso JAS (1989) Environment-specified patterns of movement coordination in normal and split-brain subjects. Exp Brain Res 75:306

Winfree A (1980) The geometry of biological time. Springer, Berlin, Heidelberg New York

Yamanishi J, Kawato M, Suzuky R (1980) Two coupled oscillators as a model for coordinated finger tapping by both hands. Biol Cybern 37:219–225